INORGANIC COMPOUNDS

Carbon content in airway macrophages and genomic instability in Chinese carbon black packers

Wenting Cheng[1] · Yuansheng Liu[1] · Jinglong Tang[1] · Huawei Duan[2] · Xiaoran Wei[1] · Xiao Zhang[2] · Shanfa Yu[3,4] · Matthew J. Campen[5] · Wei Han[6] · Nathaniel Rothman[7] · Steven A. Belinsky[8] · Qing Lan[7] · Yuxin Zheng[1] · Shuguang Leng[1]

Abstract

Carbon black (CB) particulates as virtually pure elemental carbon can deposit deep in the lungs of humans. International Agency for Research on Cancer classified CB as a Group 2B carcinogen due to inconclusive human evidence. A molecular epidemiological study was conducted in an established cohort of CB packers (CBP) to assess associations between CB exposure and genomic instability in peripheral lymphocytes using cytokinesis-block micronucleus assay (CBMN). Carbon content in airway macrophages (CCAM) was quantified as a bio-effective dosimeter for chronic CB exposure. Dose–response observed in CBPs was compared to that seen in workers exposed to diesel exhaust. The association between CB exposure status and CBMN endpoints was identified in 85 CBPs and 106 non-CBPs from a 2012 visit and replicated in 127 CBPs and 105 non-CBPs from a 2018 visit. The proportion of cytoplasm area occupied by carbon particles in airway macrophages was over fivefold higher in current CBPs compared to non-CBPs and was associated with CBMN endpoints in a dose-dependent manner. CB aerosol and diesel exhaust shared the same potency of inducing genomic instability in workers. Circulatory pro-inflammatory factors especially TNF-α was found to mediate associations between CB exposure and CBMN endpoints. In vitro functional validation supported the role of TNF-α in inducing genomic instability. An estimated range of lower limits of benchmark dose of 4.19–7.28% of CCAM was recommended for risk assessment. Chronic CB exposure increased genomic instability in human circulation and this provided novel evidence supporting its reclassification as a human carcinogen.

Keywords Carbon black · Genomic instability · Diesel exhaust · Carbon content in airway macrophages · Dose–response · Potency

Wenting Cheng, Yuansheng Liu and Jinglong Tang contributed equally.

Yuxin Zheng and Shuguang Leng co-supervised the study.

✉ Shuguang Leng
  sleng@qdu.edu.cn

[1] School of Public Health, Qingdao University, Qingdao 266021, Shandong, China

[2] National Institute for Occupational Health and Poison Control, Chinese Center for Disease Control and Prevention, Beijing, China

[3] Henan Institute of Occupational Medicine, Zhengzhou, Henan, China

[4] Henan Medical College, Zhengzhou, Henan, China

[5] College of Pharmacy, University of New Mexico, Albuquerque, NM, USA

[6] Qingdao Municipal Hospital, School of Medicine, Qingdao University, Qingdao, China

[7] Division of Cancer Epidemiology and Genetics, National Cancer Institute, National Institutes of Health, Rockville, MD, USA

[8] Lung Cancer Program, Lovelace Respiratory Research Institute, Albuquerque, NM, USA

Introductions

Carbon black [CB, CAS. No. 1333-86-4] is virtually pure elemental carbon (EC) that are produced by partial combustion or thermal decomposition of gaseous or liquid hydrocarbons under controlled conditions. Worldwide CB production

in 2012 was approximately 11 million metric tons, 90% of which was used in rubber applications (ICBA 2016). CB exposure in humans is mainly encountered through inhalation in occupational settings where CB is manufactured. CB aggregates as smallest inseparable entities deposit deep inside the lung due to its nano-scale size (100–1000 nm) (Gray and Muranko 2006) and is unlikely to be absorbed to any meaningful extent and distributed in the body (Chaudhuri et al. 2018).

International Agency for Research on Cancer (IARC) classified CB as being possibly carcinogenic to humans (Group 2B) due to inconclusive human evidence. A secondary genotoxic mechanism was proposed based on the well-known "lung overload" phenomenon observed only in rats that exposure to high doses of CB particles induced severe lung inflammation that was essential for formation of hprt mutations in airway epithelial cells and lung carcinogenesis (Chaudhuri et al. 2018; Driscoll et al. 1996, 1997). So far, no human studies have been conducted that assess whether chronic CB exposure could induce genomic instability with an established link to cancer risk.

The cytokinesis-block micronucleus (CBMN) assay detects injuries that survive at least one mitotic cycle and reflect unrepaired fixed DNA damages, i.e., mutations. A large international cohort study of 6718 healthy individuals identified strong evidences supporting increased MN formation in peripheral blood as being associated with early events in carcinogenesis (Bonassi et al. 2007). Furthermore, El-Zein et al. demonstrated that CBMN endpoints in lymphocytes with and without tobacco carcinogen challenge were significantly associated with increased lung cancer risk in a case–control study (El-Zein et al. 2006).

CCAM may be a valuable biomarker assessing lung dose of CB exposure in workers. Accumulating evidence supports carbon content in airway macrophages (CCAM) as a valid biomarker for a precise estimation of individual's exposure to airborne carbon-containing particulate matters (PM) pollution (Bai et al. 2015; Belli et al. 2016; Nwokoro et al. 2012; Whitehouse et al. 2018). Temporal studies showed that CCAM is better suited to estimate airborne carbon-containing PM levels over past six months (Jacobs et al. 2010) and has an estimated half-lives of 2–4 months (Bai et al. 2015, 2018a). CCAM has been shown to be associated with lung function (Kalappanavar et al. 2012; Kulkarni et al. 2006), cardiovascular effects (Jacobs et al. 2010, 2011), and mitochondrial DNA content in blood (Bai et al. 2018b), all well-established health endpoints for exposure to air pollution.

We conducted an epidemiological study based on an established cohort of CB baggers from an acetylene black industry and non-exposed controls to test a hypothesis that exposure to high levels of CB aerosol could increase genomic instability in peripheral lymphocytes in a dose-dependent manner and through elevating circulatory inflammation. We further compared the dose–response of CBMN frequency with CCAM to assess whether CB exposure has the potency of inducing genomic instability comparable to exposure of diesel engine exhaust (DEE), a group 1 human carcinogen.

# Study subjects and methods

Study populations

CBP study was established in 2012 by recruiting male CBPs from an acetylene black industry and male non-CBP controls from a local water authority. Design details including inclusion and exclusion criteria were published previously (Yang et al. 2019; Zhang et al. 2014). Data for CBMN endpoints were available for 85 CBPs and 106 non-CBPs enrolled at baseline among which 53 CBPs and 55 non-CBPs were successfully followed up in 2018 when new enrollment was also open to both sexes and retired workers (Supplemental Table 1). The DET study was established in 2012 under a study protocol identical to the CBP study and recruited 137 DETs and 127 non-DETs (Wang et al. 2018). Follow-up of the DET cohort was conducted in 2018 and enrolled 90 DETs and 88 non-DETs (Supplemental Tale 2), among which 51 DETs and 55 non-DETs were studied in 2012. Written informed consent was acquired from all participants prior to the interview and any procedures. The protocol was approved by the Research Ethics Committee of the National Institute for Occupational Health and Poison Control, Chinese Center for Disease Control and Prevention.

Exposure assessment

Details of exposure assessment were available in references (Dai et al. 2016a; Niu et al. 2018) and Supplemental Methods. PM2.5, PM2.5 related EC, organic carbon (OC), and total carbon (TC), and particle size distribution were assessed inside CBP and DET workshops and in control areas multiple times between 2012 and 2018 (Supplemental Table 3) (Dai et al. 2016a, b; Niu et al. 2018; Zhang et al. 2014, 2015).

CCAM assay

Sputum collection, processing, slide preparation, and quality assessment were described in detail in Supplemental Methods. Fifty randomly selected and well-stained macrophages with intact cytoplasm (Fig. 1) per subject were analyzed. The nuclei were removed prior to quantification of areas of carbon particles and cytoplasm. The proportion of cytoplasm area occupied by carbon particles (PCOC) was calculated as
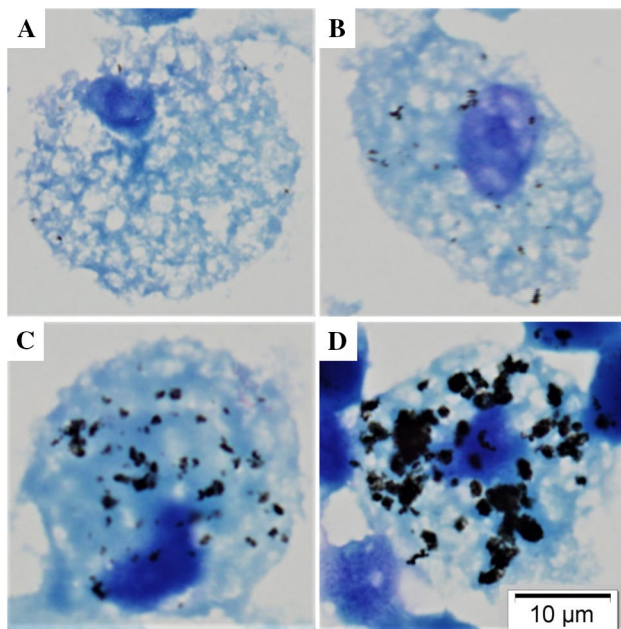
Fig. 1 Representative photos of macrophages containing different amount of carbon particles. These four well-stained macrophages were identified from a sputum sample from a female CBP. The values of CB area were 1.10, 7.65, 13.63, and 108.70 μm^2 for macrophages **a–d**, respectively. The values of PCOC were 0.65%, 1.37%, 3.45%, and 17.49% for macrophages **a–d**, respectively

a quantification of carbon content in each macrophage. The utility of PCOC may avoid biases derived from different size of macrophages and CB particles overlapping with nuclei (Bai et al. 2015; Frankenberger et al. 2004). Mean, median, and quartiles of PCOC from 50 macrophages per individual were calculated and analyzed for their associations with CB exposure status which facilitate biomarker selection for subsequent analyses.

CBMN assay

The assay was conducted in batches according to our previous studies (Duan et al. 2009; Leng et al. 2004; Thomas and Fenech 2011; Zhang et al. 2015). Slides were scored according to criteria outlined in HUMN Project (Fenech et al. 2003). Detailed description is available in Supplemental Methods.

Circulatory inflammatory markers

Interleukin (IL)-1β, IL-6, tumor necrosis factor (TNF)-α, IL-8, macrophage inflammatory protein (MIP)-1β, and C-reactive protein (CRP) were measured in serum samples collected in 2012 (Dai et al. 2016c).

Statistical analysis

The associations between CB exposure status or PCOC and CBMN endpoints were assessed using Poisson regression. Generalized linear model (GLM) was used to assess the associations of PCOC and pro-inflammatory factors with CB exposure status. We pooled databases of CBP and DET studies to determine if slopes of linear curves between PCOC and CBMN endpoints varied between studies. Mediation analysis assessed the effect of circulatory inflammation on the association between CB exposure and CBMN endpoints (Fig. 2a). Benchmark dose (BMD) and its lower bound (BMDL) of PCOC associated with a benchmark response (BMR) of genomic instability was estimated (Wang et al. 2018). Detailed descriptions were available in Supplemental Methods.

Results

Ambient exposure assessment

Up to 99.6% CB particles had aerodynamic diameter less than 2.5 μm with 96.7% particles less than 1.0 μm (Dai et al. 2016a). Average PM2.5 level inside CB bagging facilities in the fall of 2012 was 800 μg/m^3 with PM2.5 related EC level of 657.0 μg/m^3 (Supplemental Table 3) (Dai et al. 2016a). In the fall of 2018, geometric mean of PM2.5 level in CB bagging areas was 637.4 μg/m^3 with PM2.5 related EC level of 364.6 μg/m^3. The EC/TC ratio was above 92.5% in both visits, consistent with the fact that CB is almost pure EC (Dai et al. 2016a).

Characteristics of study subjects

At baseline, CBPs had distribution of all demographic variables similar to non-CBP controls (all *P* values > 0.11, Supplemental Table 1). At follow-up, current CBPs (CBP-C) had more males, more current smokers, and fewer pack years consumed in current smokers compared to non-CBPs. Former CBPs (CBP-F) were older and had longer exposure history with a median retirement of 3.7 years.

CCAM in sputum from CBPs and non-CBPs

Among 232 cohort members with CBMN data studied in 2018, 44 CBP-Cs, 40 CBP-Fs, and 64 non-CBPs provided sputum samples sufficient for CCAM analysis (Fig. 3). PCOC levels were 5.3- to 6.2-fold higher in CBP-Cs than non-CBPs (Supplemental Table 4). CBP-Fs had lower level of PCOC compared to CBP-Cs, however, still much higher than that seen in non-CBPs (2.9- to 3.4-fold higher, Supplemental Table 4). In addition, time since retirement was

A

The proportion mediated = (c-c') / c

B

C

D
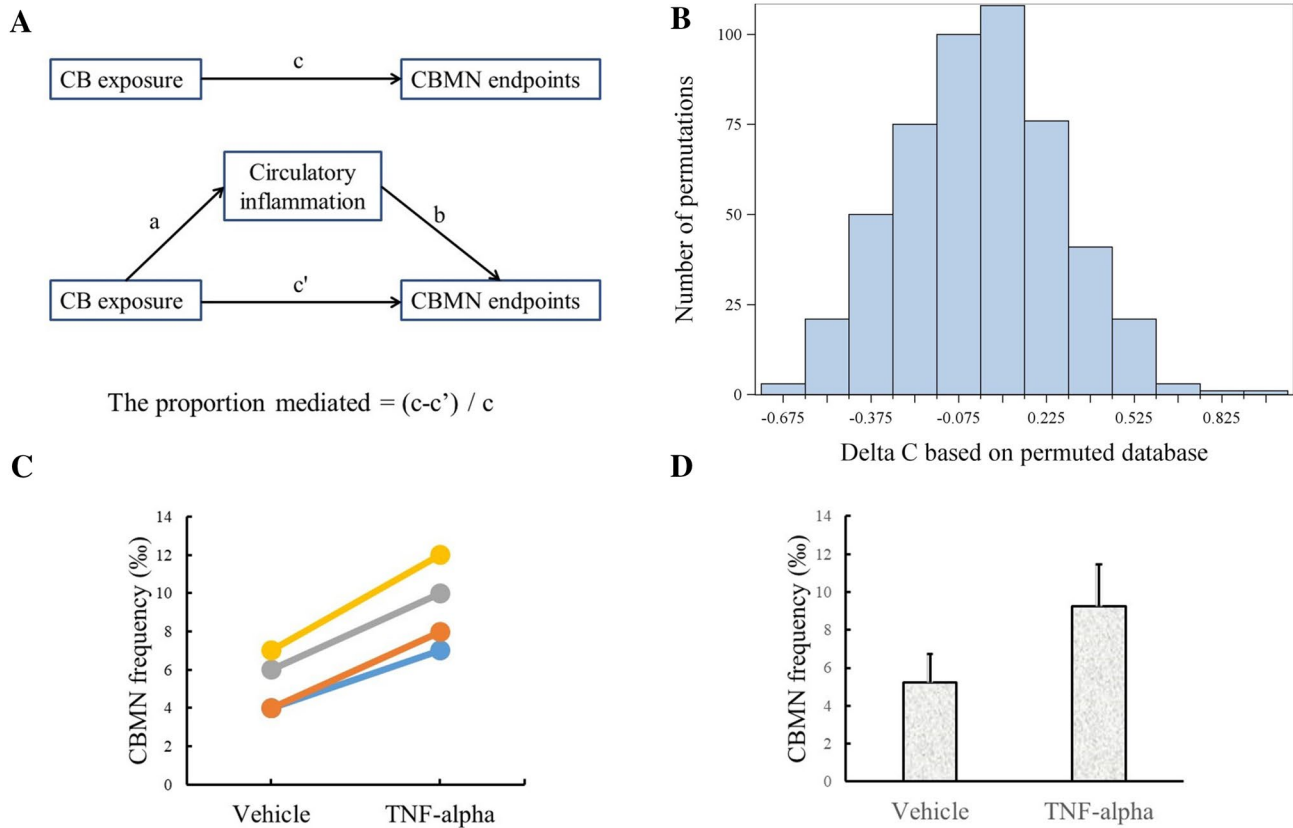
Fig. 2 Circulatory inflammation mediating CB exposure induced genomic instability. In mediation analysis (**a**), the *c* coefficient denotes direct effect of CB exposure on CBMN endpoints, without controlling for circulatory inflammation (mediator). The *c'* coefficient denotes direct effect of CB exposure on CBMN endpoints, controlling for circulatory inflammation (mediator). The proportion mediated is equal to delta *c* (i.e., *c–c'*) divided by *c*. We took a permutation-based method to assess whether the proportion mediated was statistically significant or not (**b**). The relationship between NPB and the vector of independent variables was permuted for 500 times. Each permutated database allowed the association analysis of NPB with CB

exposure and other covariates without and with TNF-α to calculate the *c* and *c'*. Permutation was conducted for 500 times to generate a distribution of *c–c'* under null hypothesis of no mediation. Value of *c–c'* calculated using observed data (0.554) was compared to the distribution generated by permutation and P_{perm} was calculated as the number of permuted databases generating a *c–c'* that is greater than observed value (*n* = 10 for TNF-α) divided by 500. In vitro functional validation identified TNF-α treatment at a physiological relevant dose (1.44 ng/ml) significantly increased CBMN frequency (*P* = 0.0023), supporting the role of TNF-α as a mediator for CB exposure induced genomic instability (**c**, **d**)

inversely associated with PCOC (all Ps < 0.021, Supplemental Fig. 1, not shown). Because Q3 (i.e., 75 percentile) of PCOC does not contain zero values and has the widest distribution in studied subjects, it was selected for all additional data analyses.

Effects of CB exposure status on CBMN endpoints

CBP-Cs had significantly higher frequencies of MN, nucleoplasmic bridges (NPB), nuclear bud (BUD), and CBMN compared to non-CBPs in both baseline and follow-up visits (Table 1). In addition, in 2018 visit CBP-Fs had an increasing trend for all CBMN endpoints compared to non-CBPs, although frequency ratios (FR) were smaller than that seen for CBP-Cs. Time since retirement was inversely associated with BUD and CBMN frequencies (all *P* values < 0.023,

Supplemental Fig. 2). Additional analyses showed that the effect of CB exposure on CBMN endpoints did not vary by smoking status (all *P* values > 0.13, not shown), supporting no potential confounding effects of cigarette smoking.

A dose–response relationship between CCAM and CBMN endpoints

The scatter plots between Q3 of PCOC with and without natural log transformation and CBMN endpoints suggest a dose-dependent linear relationship (Fig. 4a–d and Supplemental Fig. 3A–D). Poisson regression identified every 10% increase in Q3 of PCOC associated with 18%, 32%, 24% and 21% increased FRs for MN, NPB, BUD and CBMN frequencies in 147 study subjects (Supplemental Table 5). Similar associations were observed as well when CBP-Fs
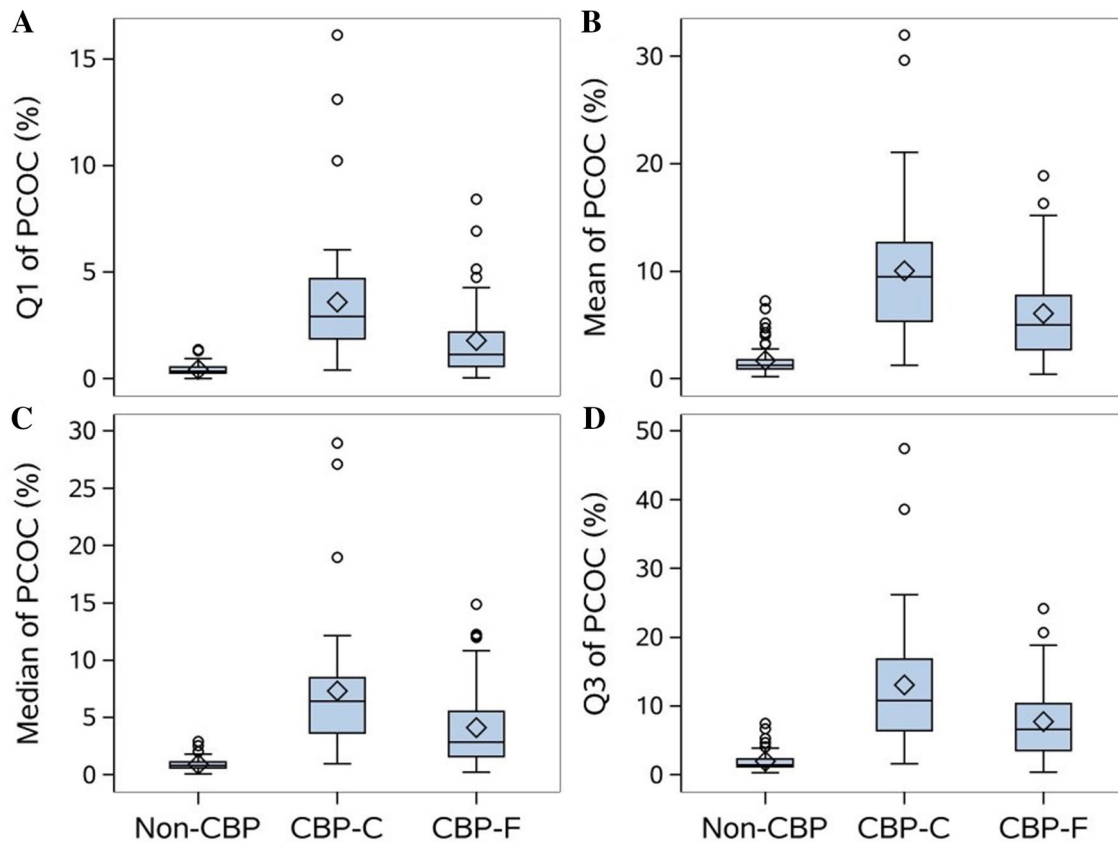
Fig. 3 Box plots of PCOC by exposure statuses in CBP study. For each individual, Q1, mean, median, and Q3 were calculated from PCOC measurements of 50 airway macrophages as the CCAM readouts for that subject. The distributions of these four measurements in 63 non-CBPs, 44 CBP-Cs, and 40 CBP-Fs were shown and the levels of PCOC were 5.3–6.2-fold higher in CBP-Cs than non-CBPs.

CBP-Fs had lower level of PCOC compared to CBP-Cs, however, still much higher than that seen in non-CBPs (2.9–3.4-fold higher). Q3 of PCOC does not contain zero values and has the widest distribution in studied subjects. The five horizontal bars from bottom to top represent the minimum, first quartile, median, third quartile, and maximum. Open diamond represents mean. Outliers are shown in circles

were excluded or when analyses were restricted in CBPs only (Supplemental Table 5). In addition, the association between Q3 of PCOC and CBMN endpoints did not vary by smoking status (all P values > 0.66, not shown).

Comparison of potency for inducing genomic instability between CB aerosol and DEE

Our own analysis of CB and diesel exhaust particles (DEP) collected from the field and others identified considerable similarity in primary sphere diameter, high surface area per mass values, and aciniform morphology, though DEPs tend to form smaller aggregates and agglomerates and contain high percentage of OC (56.0%) compared to CB (Supplemental Fig. 4) (Dai et al. 2016a; Long et al. 2013; Niu et al. 2018). Follow-up of the DET cohort in 2018 enrolled 90 DETs and 88 non-DETs (Supplemental Table 2). A significant increase in all CBMN endpoints was identified in DETs versus non-DETs (Supplemental Table 6), replicating the results of baseline study (Zhang et al. 2015). In addition,

CCAM was successfully measured in 64 DETs and 61 non-DETs (Supplemental Table 7 and Supplemental Fig. 5). A dose-dependent, monotonic increase in MN and CBMN frequencies with an increasing level of Q3 of PCOC was shown in the scatter plots (Supplemental Fig. 6). Poisson regression identified that every 10% increase in Q3 of PCOC associated with 28% and 20% increased FRs for MN and CBMN frequencies in 125 study subjects (Supplemental Table 8).

We pooled the data of the CBP and DET studies to compare the potency for inducing genomic instability between exposures to CB aerosol and DEE. As shown in Fig. 5a and Supplemental Fig. 7a, the dose–response curves of CBMN frequency with Q3 of PCOC with and without natural log transformation were parallel between CBP and DET studies and this was also supported by the interaction analysis between Q3 of PCOC and study identification for affecting CBMN frequency, which was not significant (Table 2). In addition, although the dose–response curves of MN frequency with Q3 of PCOC with and without natural log transformation seemed to be a little steeper in DET versus CBP

Table 1 Effects of CB exposure on CBMN endpoints in the field visits of 2012 and 2018

Variable	Non-CBP	CBP-C	CBP-F	FR1 (95% CI)	FR2 (95% CI)
Field visit in 2012					
MN (‰)	4.53 ± 3.00	8.19 ± 5.99		1.78 (1.45–2.18)[a]	
NPB (‰)	0.29 ± 0.70	0.51 ± 0.95		1.94 (1.13–3.32)[c]	
BUD (‰)	0.89 ± 1.26	2.62 ± 2.13		3.09 (2.22–4.29)[a]	
CBMN (‰)	5.66 ± 3.59	11.29 ± 6.88		1.99 (1.65–2.41)[a]	
NDI	1.82 ± 0.16	1.79 ± 0.17			
Field visit in 2018					
MN (‰)	6.11 ± 2.74	7.16 ± 3.63	6.95 ± 3.30	1.24 (1.06–1.46)[b]	1.11 (0.94–1.32)
NPB (‰)	0.46 ± 0.81	0.74 ± 1.35	0.60 ± 0.78	1.59 (0.97–2.61)[d]	1.23 (0.69–2.61)
BUD (‰)	4.38 ± 2.70	6.26 ± 3.40	5.05 ± 2.55	1.50 (1.25–1.81)[a]	1.17 (0.95–1.44)[e]
CBMN (‰)	10.95 ± 4.70	14.16 ± 6.76	12.60 ± 5.22	1.36 (1.18–1.58)[a]	1.14 (0.97–1.34)
NDI	1.40 ± 0.16	1.44 ± 0.23	1.46 ± 0.18		
Apoptosis (%)	12.88 ± 6.97	17.12 ± 8.94[b]	15.82 ± 7.23[f]		
Necrosis (%)	8.95 ± 4.68	8.53 ± 4.60	9.68 ± 5.25		

Poisson regression examined the association between CB exposure and CBMN endpoints with adjustment for age, BMI, current smoking and drinking status, and packyears in 2012 and 2018 studies separately. Frequency ratio (95% CIs) was calculated from regression coefficients for CB exposure status, β, through the equation $FR = e^{\beta}$. CBMN endpoints were summarized as Mean ± SD. FR1 quantified the magnitude of association in CBP-Cs versus non-CBPs, whereas FR2 quantified the magnitude of association in CBP-Fs versus non-CBPs. Sample sizes for non-CBPs and CBPs in 2012 were 106 and 85 for MN, and 92 and 81 for NPB, BUD, and CBMN, respectively

MN micronucleus, *NPB* nucleoplasmic bridge, *BUD* nuclear bud, *NDI* nuclear division index, *CBP* carbon black packer, *CBP-C* current CBP, *CBP-F* former CBP, *FR* frequency ratio

[a]Compared to non-CBPs, $P < 0.0001$

[b]Compared to non-CBPs, $P < 0.01$

[c]Compared to non-CBPs, $P < 0.05$

[d]Compared to non-CBPs, $P = 0.065$

[e]Compared to CBP-Cs, $P = 0.068$

[f]Compared to non-CBPs, $P = 0.054$

studies (Fig. 5b and Supplemental Fig. 7b), the difference in slopes was not statistically significant (Table 2). These results suggested that the potencies of inducing genomic instability between CB aerosol and DEE were not different.

Circulatory inflammation mediating the effect of CB exposure on CBMN endpoints

Many pro-inflammatory factors could promote carcinogenesis by inducing the formation of reactive nitrogen/oxygen species and inhibiting DNA repair machinery that together contribute to elevated genotoxicity and mutation frequency (Jaiswal et al. 2000; Yan et al. 2006). Our study found that serum TNF-α, IL-1β and IL-6 had highest folds of increase (7.0–10.6-fold) in CBPs versus non-CBP controls followed by MIP-1β (3.3-fold) and CRP (2.7-fold, Supplemental Table 9), consistent with our previous study (Zhang et al. 2014). We further assessed whether CB exposure could affect the CBMN endpoints through increasing the circulatory inflammation using mediation analysis (Fig. 2a). Analyses identified evidence to support IL-6, TNF-α, MIP-1β, and

IL-1β as a mediator with TNF-α having a mediation effect for all three endpoints (Table 3 and Fig. 2a, b). The highest degree of mediation effect was observed for TNF-α that mediated 75.4% of the magnitude of the association between CB exposure and NPB formation. We further conducted an in vitro functional validation experiment in which four PHA-stimulated lymphocyte cultures were treated with a physiologically relevant dose of TNF-α (1.44 ng/ml) for 48 h prior to harvest. Excitingly, CBMN frequency increased from 5.3 ± 1.5‰ in vehicle control to 9.3 ± 2.2‰ with TNF-α treatment ($P = 0.0023$), supporting TNF-α as a mediator for CB exposure induced genomic instability (Fig. 2c, d).

BMD and BMDL estimation

Because no difference in potency of inducing genomic instability between CB aerosol and DEE was observed, study subjects ($n = 274$) of CBP and DET studies were pooled to estimate BMD and BMDL. Study subjects were categorized into four groups based on exposure status and PCOC (Supplemental Table 10). The 90th percentile of CBMN frequency
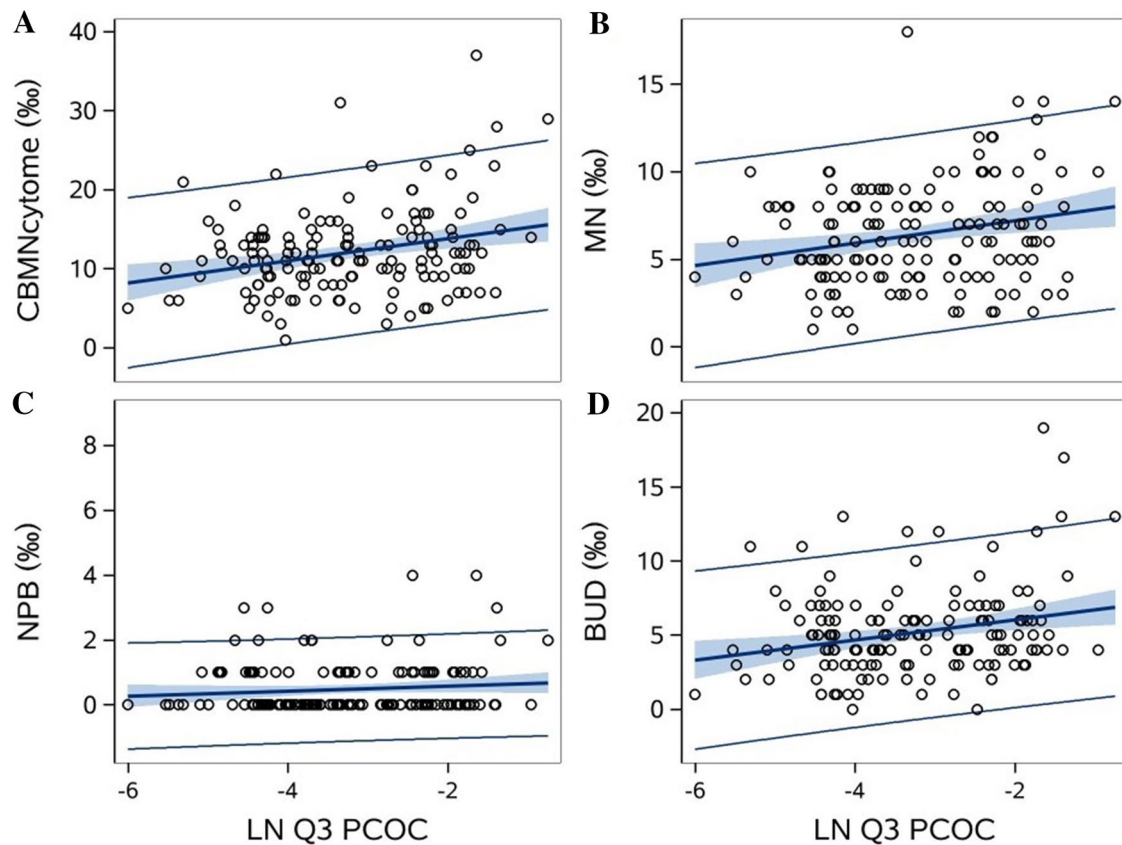
Fig. 4 Scatter plots between natural log transformed Q3 of PCOC and CBMN endpoints. These scatter plots suggest a dose-dependent linear relationship between natural log transformed Q3 of PCOC and all CBMN endpoints in 64 non-CBPs and 84 CBPs

in controls (15‰) was set as the cut point to define a subject having high genomic instability. A monotonically increasing dose–response pattern was identified between the PCOC category and rate of having increased genomic instability (Supplemental Table 10). Eight models were assessed to fit the dose–response and Log–Logistic model generated the lowest AIC indicative of the best model fitness (Supplemental Fig. 8 and Supplemental Table 11). The BMD and BMDL of Q3 of PCOC were 6.26% and 4.17%.

Discussion

Our study found that chronic exposure to a high level of CB aerosol (EC level 364.6–657.0 µg/m³) dramatically increased genomic instability in peripheral lymphocytes of CB baggers, a validated biomarker predicting cancer risk (Bonassi et al. 2007; El-Zein et al. 2006). Moreover, we confirmed a dose-dependent monotonic increase in genomic instability with increasing levels of PCOC in sputum that was independent of smoking status. Furthermore, CB aerosol exposure had potency of inducing genomic instability similar to that seen for DEE exposure, an established human

carcinogen. This is consistent with previous findings that inhalation of DEE, which contains carbonaceous cores with adsorbed mutagenic organic compounds, and its virtually mutagen-free carbonaceous core analog, CB, produce similar histological and molecular types and prevalence of pulmonary neoplasms in chronically exposed F344 rats (Nikula et al. 1995; Swafford et al. 1995). These novel findings provide strong evidence in humans that could contribute to the escalation of the classification of CB carcinogenicity.

Previous animal studies found that CB exposure may cause gene mutations in lung cells through an inflammation-mediated genotoxic mechanism (Chaudhuri et al. 2018). We recapitulated this finding in humans that chronic exposure to CB aerosol increased genomic instability principally through elevating circulatory inflammation. Among factors tested, TNF-α showed consistent mediation effect across all CBMN endpoints. TNF-α at a pharmacological dose (50 ng/ml) behaves like a potent mutagen through inducing reactive oxygen species in mammalian cells (Yan et al. 2006). Moreover, increase of TNF-α levels in blood by hydrodynamic delivery of a TNF-α expression plasmid could also induce 8-OHdG in mouse liver tissue (Yan et al. 2006). Our in vitro functional validation also found that a physiologically
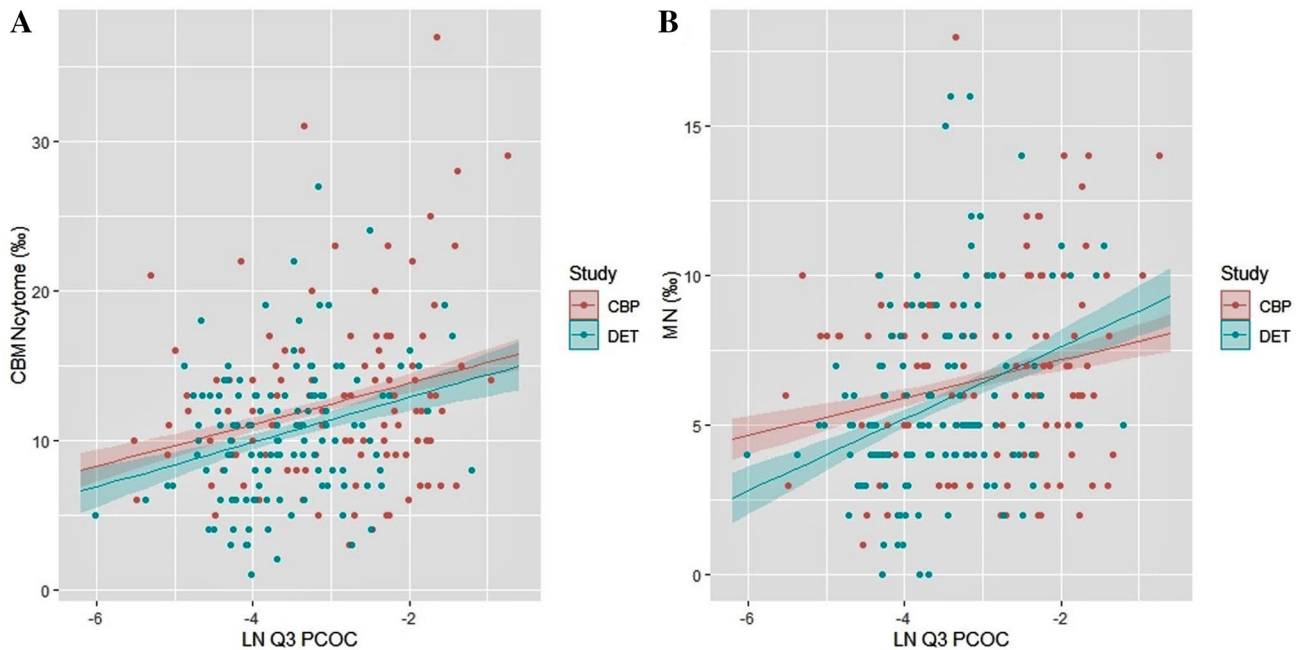
Fig. 5 Comparison of dose–response of CBMN endpoints with natural log transformed Q3 of PCOC between CBP and DET studies. Slopes of linear dose–response curves were compared between CBP and DET studies. Linear curve of CBMN frequency with natural log transformed Q3 of PCOC in CBP study was in parallel with that seen in DET study (**a**). Linear curves of MN frequency with natural log transformed Q3 of PCOC seemed to be steeper in DET versus CBP studies (**b**). Slopes were compared by including an interaction term between study ID and natural log transformed Q3 of PCOC in Poisson regression. The interaction term was not statistically significant, suggesting CB aerosol had similar potency in including genomic instability compared to DEE

Table 2 The comparison of potency for inducing genomic instability between CB aerosol and DEE in the visit of 2018

Endpoint	Independent variable (PCOC)		PCOC		Study ID		Interaction term	
	Label	Unit of change	FR (95% CI)	P	FR (95% CI)	P	FR (95% CI)	P
CBMN	Q3	10%	1.21 (1.11–1.31)	<0.0001	1.00 (0.98–1.02)	0.82	0.99 (0.83–1.18)	0.88
MN	Q3	10%	1.17 (1.06–1.29)	0.0012	1.00 (0.98–1.02)	0.96	1.08 (0.89–1.31)	0.42
CBMN	LN Q3	2.72-fold	1.41 (1.17–1.69)	0.0002	0.95 (0.32–2.87)	0.93	0.99 (0.73–1.35)	0.94
MN	LN Q3	2.72-fold	1.38 (1.12–1.69)	0.0024	2.14 (0.63–7.23)	0.22	1.21 (0.86–1.70)	0.27

Poisson regression examined the association between Q3 of PCOC and CBMN and MN frequencies with adjustment for age, BMI, current smoking and drinking status, and pack-years in 147 subjects from the CBP study and 125 subjects from the DET study

MN micronucleus, *CBMN* cytokinesis block micronucleus, *Q3* 75th quartile, *LN* natural log, *FR* frequency ratio, *PCOC* proportion of cytoplasm area occupied by carbon particles, *FR* frequency ratio

relevant dose of TNF-α (1.44 ng/ml) approximately doubled the CBMN frequency seen in untreated lymphocytes, supporting the role of TNF-α as a mediator for CB exposure induced genomic instability.

Although CB aerosol and DEE shared similar potency of inducing genomic instability in workers, underlying mechanisms may be different. DEE exposure showed a much weaker induction of inflammatory factors in circulation (Supplemental Table 9, (Dai et al. 2016b). No circulatory factors were identified to mediate the association between DEE exposure and CBMN endpoints (not shown,

Zhang et al. 2015). Polycyclic aromatic hydrocarbons and nitropyrenes absorbed on carbonaceous cores have been suggested as principal mutagenic and carcinogenic constituents of inhaled DEE (Grimmer et al. 1987). Thus, the mechanism underlying observed dose–response in DET study may be more relevant to mutagenic constituents carried by carbonaceous core in DEE.

PCOC in airway macrophages provided a fully quantitative measure for lung EC burden as a bio-effective dosimeter for exposure to CB aerosol. Our study pooled current and former CBPs together and projected a half-life of 7 years for

Table 3 Mediation effect of circulatory inflammation on associations between CB exposure and CBMN endpoints in the visit of 2012

CBMN	Inflammation	IQR in non-CBPs	Inflammation—CBMN			CB exposure—CBMN[a]			Mediation effect[b]	
			estimate (SE)	FR	P	estimate (SE)	FR	P	PM	P_{perm}
MN	IL-6 (pg/ml)	52.1	0.053 (0.016)	1.054	0.0012	0.393 (0.119)	1.481	0.0010	0.322	0.018
	TNF-α (pg/ml)	94.3	0.081 (0.038)	1.084	0.031	0.424 (0.128)	1.528	0.0009	0.269	0.064
	MIP-1β (ng/ml)	1.05	− 0.017 (0.023)		0.45	0.620 (0.116)		< 0.0001	NM	
	IL-1β (pg/ml)	6.2	0.016 (0.014)		0.26	0.563 (0.105)		< 0.0001	NM	
	CRP (mg/l)	0.75	0.015 (0.012)		0.19	0.551 (0.107)		< 0.0001	NM	
NPB	IL-6 (pg/ml)	52.1	0.016 (0.045)		0.73	0.681 (0.321)		0.034	NM	
	TNF-α (pg/ml)	94.3	0.252 (0.080)	1.287	0.0016	0.181 (0.340)	1.198	0.60	0.754	0.020
	MIP-1β (ng/ml)	1.05	0.088 (0.031)	1.092	0.0042	0.434 (0.304)	1.543	0.15	0.410	0.032
	IL-1β (pg/ml)	6.2	0.185 (0.063)	1.203	0.0035	0.372 (0.310)	1.451	0.23	0.494	0.024
	CRP (mg/l)	0.75	0.023 (0.024)		0.33	0.679 (0.287)		0.018	NM	
BUD	IL-6 (pg/ml)	52.1	0.016 (0.025)		0.51	1.091 (0.192)		< 0.0001	NM	
	TNF-α (pg/ml)	94.3	0.124 (0.048)	1.132	0.0098	0.895 (0.199)	2.447	< 0.0001	0.220	0.044
	MIP-1β (ng/ml)	1.05	0.0003 (0.026)		0.99	1.147 (0.185)		< 0.0001	NM	
	IL-1β (pg/ml)	6.2	0.0043 (0.043)		0.92	1.140 (0.186)		< 0.0001	NM	
	CRP (mg/l)	0.75	0.0104 (0.015)		0.49	1.125 (0.174)		< 0.0001	NM	

Non-transformed data of cytokine and chemokine levels were used in Poisson regression. Sample sizes were 105 (non-CBPs)/84 (CBPs) for MN association analysis and 92/81 for NPB and BUD association analyses

MN micronucleus, *NPB* nucleoplasmic bridge, *BUD* nuclear bud, *CBMN* cytokinesis block micronucleus, *IQR* inter quartile range, *SE* standard error, *FR* frequency ratio, *PM* the proportion mediated effect size

[a]The estimates for CB exposure for affecting MN, NPB, and BUD frequencies were 0.580 (SE = 0.104, $P < 0.0001$), 0.735 (SE = 0.279, $P = 0.0083$), and 1.148 (SE = 0.171, $P < 0.0001$), respectively when the model did not include cytokines or chemokines

[b]The proportion mediated effect size that quantifies the proportion of a total effect that is mediated was calculated using the following equation: $(C–C')/C$. The database was permuted for 500 times to generate a null distribution of $C–C'$ (Fig. 2). P_{perm} was calculated as the number of permuted databases generating a $C–C'$ that is greater than observed value divided by 500

CB clearance in airway macrophages after retirement (Supplemental Fig. 1), which seems much longer than half-lives of 2–4 months reported in a panel of migrants from China and India with annual PM10 > 50 μg/m³ to Belgium with annual PM10 of < 30 μg/m³ (Bai et al. 2015, 2018a). However, it is important to note that declining rate of CB areas in airway macrophages was estimated to be 0.0060 μm² per day in our study which was consistent to values (0.006 and 0.0013 μm²/day) reported before (Bai et al. 2015, 2018a). Thus, elongated half-life may be mainly due to high CCAM levels in active CBPs that decline at a relatively consistent rate after retirement. Furthermore, declining rate of CCAM (9.5%) after retirement was very close to that seen for CBMN frequencies (7.8%), further suggesting these two events sharing similar clearance kinetics. This premise is further supported by significant associations between Q3 of PCOC and CBMN endpoints in current and former CBPs combined (Supplemental Table 5). Thus, the assessment of CCAM in CB exposed populations provided a reliable dosimetry using engulfed CB in airway macrophages, a pivotal immunological component mediating inflammatory response in the lungs with secreted inflammatory factors translocatable into systemic circulation (Kido et al. 2011; Tamagawa et al. 2009).

Our study has additional strengths. First, we used a two-stage design to identify a consistent association between CB exposure and genomic instability. Excluding the subjects from the 2018 visit who were also studied at baseline, similar association between CB exposure status and CBMN endpoints remained (not shown). Second, a combination of mediation analysis and functional validation substantiates our mechanistic interpretation.

Our study has limitations. First, we could not completely exclude the possibility that the association between CB exposure and genomic instability may be underestimated due to healthy worker effect in which susceptible workers would have left due to elevated inflammation related health issues. Second, not all study subjects provided a sufficient sputum sample for CCAM analysis. However, our successful rate of 67% is consistent with other studies (Bai et al. 2015). Moreover, it is unlikely that dose–response observed could not be generalized to entire study populations because comparison of relevant variables between subjects with and without a successful induction identified no differences.

Conclusions

Using a unique cohort of carbon black baggers, we identified novel and strong evidence in humans that could support the escalation of the classification of CB carcinogenicity. In addition, for regulatory purpose in workers exposed to carbon-containing PMs, we estimated a range of BMDLs of PCOC (4.19–7.28%) in sputum for not having extra risk of genomic instability.

Compliance with ethical standards

Conflict of interest The authors declare that they have no conflict of interest.

References

Bai Y, Brugha RE, Jacobs L, Grigg J, Nawrot TS, Nemery B (2015) Carbon loading in airway macrophages as a biomarker for individual exposure to particulate matter air pollution—a critical review. Environ Int 74:32–41. https://doi.org/10.1016/j.envint.2014.09.010

Bai Y, Bove H, Nawrot TS, Nemery B (2018a) Carbon load in airway macrophages as a biomarker of exposure to particulate air pollution; a longitudinal study of an international panel. Part Fibre Toxicol 15(1):14. https://doi.org/10.1186/s12989-018-0250-8

Bai Y, Casas L, Scheers H, Janssen BG, Nemery B, Nawrot TS (2018b) Mitochondrial DNA content in blood and carbon load in airway macrophages. A panel study in elderly subjects. Environ Int 119:47–53. https://doi.org/10.1016/j.envint.2018.06.003

Belli AJ, Bose S, Aggarwal N et al (2016) Indoor particulate matter exposure is associated with increased black carbon content in airway macrophages of former smokers with COPD. Environ Res 150:398–402. https://doi.org/10.1016/j.envres.2016.06.025

Bonassi S, Znaor A, Ceppi M et al (2007) An increased micronucleus frequency in peripheral blood lymphocytes predicts the risk of cancer in humans. Carcinogenesis 28(3):625–631. https://doi.org/10.1093/carcin/bgl177

Chaudhuri I, Fruijtier-Polloth C, Ngiewih Y, Levy L (2018) Evaluating the evidence on genotoxicity and reproductive toxicity of carbon black: a critical review. Crit Rev Toxicol 48(2):143–169. https://doi.org/10.1080/10408444.2017.1391746

Dai Y, Niu Y, Duan H et al (2016a) Effects of occupational exposure to carbon black on peripheral white blood cell counts and lymphocyte subsets. Environ Mol Mutagen 57(8):615–622. https://doi.org/10.1002/em.22036

Dai Y, Zhang X, Zhang R et al (2016b) Long-term exposure to diesel engine exhaust affects cytokine expression among occupational population. Toxicol Res 5(2):674–681. https://doi.org/10.1039/c5tx00462d

Dai Y, Zhang X, Zhang R et al (2016c) Long-term exposure to diesel engine exhaust affects cytokine expression among occupational population. Toxicol Res 5(2):674–681. https://doi.org/10.1039/c5tx00462d

Driscoll KE, Carter JM, Howard BW et al (1996) Pulmonary inflammatory, chemokine, and mutagenic responses in rats after subchronic inhalation of carbon black. Toxicol Appl Pharmacol 136(2):372–380. https://doi.org/10.1006/taap.1996.0045

Driscoll KE, Deyo LC, Carter JM, Howard BW, Hassenbein DG, Bertram TA (1997) Effects of particle exposure and particle-elicited inflammatory cells on mutation in rat alveolar epithelial cells. Carcinogenesis 18(2):423–430. https://doi.org/10.1093/carcin/18.2.423

Duan H, Leng S, Pan Z et al (2009) Biomarkers measured by cytokinesis-block micronucleus cytome assay for evaluating genetic damages induced by polycyclic aromatic hydrocarbons. Mutat Res 677(1–2):93–99. https://doi.org/10.1016/j.mrgentox.2009.06.002

El-Zein RA, Schabath MB, Etzel CJ, Lopez MS, Franklin JD, Spitz MR (2006) Cytokinesis-blocked micronucleus assay as a novel biomarker for lung cancer risk. Can Res 66(12):6449–6456. https://doi.org/10.1158/0008-5472.CAN-06-0326

Fenech M, Chang WP, Kirsch-Volders M et al (2003) HUMN project: detailed description of the scoring criteria for the cytokinesis-block micronucleus assay using isolated human lymphocyte cultures. Mutat Res 534(1–2):65–75. https://doi.org/10.1016/s1383-5718(02)00249-8

Frankenberger M, Menzel M, Betz R et al (2004) Characterization of a population of small macrophages in induced sputum of patients with chronic obstructive pulmonary disease and healthy volunteers. Clin Exp Immunol 138(3):507–516. https://doi.org/10.1111/j.1365-2249.2004.02637.x

Gray CA, Muranko H (2006) Studies of robustness of industrial aciniform aggregates and agglomerates—carbon black and amorphous silicas: a review amplified by new data. J Occup Environ Med 48(12):1279–1290. https://doi.org/10.1097/01.jom.0000251477.40643.2a

Grimmer G, Brune H, Deutsch-Wenzel R et al (1987) Contribution of polycyclic aromatic hydrocarbons and nitro-derivatives to the carcinogenic impact of diesel engine exhaust condensate evaluated by implantation into the lungs of rats. Cancer Lett 37(2):173–180. https://doi.org/10.1016/0304-3835(87)90160-1

ICBA (2016) Carbon black user's guide. http://www.carbon-black.org/images/docs/2016-ICBA-Carbon-Black-User-Guide.pdf

Jacobs L, Emmerechts J, Mathieu C et al (2010) Air pollution related prothrombotic changes in persons with diabetes. Environ Health Perspect 118(2):191–196. https://doi.org/10.1289/ehp.0900942

Jacobs L, Emmerechts J, Hoylaerts MF et al (2011) Traffic air pollution and oxidized LDL. PLoS ONE 6(1):e16200. https://doi.org/10.1371/journal.pone.0016200

Jaiswal M, LaRusso NF, Burgart LJ, Gores GJ (2000) Inflammatory cytokines induce DNA damage and inhibit DNA repair in cholangiocarcinoma cells by a nitric oxide-dependent mechanism. Cancer Res 60(1):184–190

Kalappanavar NK, Vinodkumar CS, Gouli C et al (2012) Carbon particles in airway macrophage as a surrogate marker in the early detection of lung diseases. Int J Occup Environ Med 3(2):68–75

Kido T, Tamagawa E, Bai N et al (2011) Particulate matter induces translocation of IL-6 from the lung to the systemic circulation. Am J Respir Cell Mol Biol 44(2):197–204. https://doi.org/10.1165/rcmb.2009-0427OC

Kulkarni N, Pierse N, Rushton L, Grigg J (2006) Carbon in airway macrophages and lung function in children. N Engl J Med 355(1):21–30. https://doi.org/10.1056/NEJMoa052972

Leng S, Dai Y, Niu Y et al (2004) Effects of genetic polymorphisms of metabolic enzymes on cytokinesis-block micronucleus in peripheral blood lymphocyte among coke-oven workers. Cancer Epidemiol Biomark Prev 13(10):1631–1639

Long CM, Nascarella MA, Valberg PA (2013) Carbon black vs. black carbon and other airborne materials containing elemental carbon: physical and chemical distinctions. Environ Pollut 181:271–286. https://doi.org/10.1016/j.envpol.2013.06.009

Nikula KJ, Snipes MB, Barr EB, Griffith WC, Henderson RF, Mauderly JL (1995) Comparative pulmonary toxicities and carcinogenicities of chronically inhaled diesel exhaust and carbon black in F344 rats. Fundam Appl Toxicol 25(1):80–94

Niu Y, Zhang X, Meng T et al (2018) Exposure characterization and estimation of benchmark dose for cancer biomarkers in an occupational cohort of diesel engine testers. J Expo Sci Environ Epidemiol 28(6):579–588. https://doi.org/10.1038/s41370-018-0061-x

Nwokoro C, Ewin C, Harrison C et al (2012) Cycling to work in London and inhaled dose of black carbon. Eur Respir J 40(5):1091–1097. https://doi.org/10.1183/09031936.00195711

Swafford DS, Nikula KJ, Mitchell CE, Belinsky SA (1995) Low frequency of alterations in p53, K-ras, and mdm2 in rat lung neoplasms induced by diesel exhaust or carbon black. Carcinogenesis 16(5):1215–1221. https://doi.org/10.1093/carcin/16.5.1215

Tamagawa E, Suda K, Wei Y et al (2009) Endotoxin-induced translocation of interleukin-6 from lungs to the systemic circulation. Innate Immun 15(4):251–258. https://doi.org/10.1177/1753425909104782

Thomas P, Fenech M (2011) Cytokinesis-block micronucleus cytome assay in lymphocytes. Methods Mol Biol 682:217–234. https://doi.org/10.1007/978-1-60327-409-8_16

Wang H, Duan H, Meng T et al (2018) Local and systemic inflammation may mediate diesel engine exhaust-induced lung function impairment in a Chinese occupational cohort. Toxicol Sci 162(2):372–382. https://doi.org/10.1093/toxsci/kfx259

Whitehouse AL, Miyashita L, Liu NM et al (2018) Use of cleaner-burning biomass stoves and airway macrophage black carbon in Malawian women. Sci Total Environ 635:405–411. https://doi.org/10.1016/j.scitotenv.2018.04.125

Yan B, Wang H, Rabbani ZN et al (2006) Tumor necrosis factor-alpha is a potent endogenous mutagen that promotes cellular transformation. Cancer Res 66(24):11565–11570. https://doi.org/10.1158/0008-5472.CAN-06-2540

Yang M, Li Y, Meng T et al (2019) Ultrafine CB-induced small airway obstruction in CB-exposed workers and mice. Sci Total Environ 671:866–873. https://doi.org/10.1016/j.scitotenv.2019.03.033

Zhang R, Dai Y, Zhang X et al (2014) Reduced pulmonary function and increased pro-inflammatory cytokines in nanoscale carbon black-exposed workers. Part Fibre Toxicol 11:73. https://doi.org/10.1186/s12989-014-0073-1

Zhang X, Duan H, Gao F et al (2015) Increased micronucleus, nucleoplasmic bridge, and nuclear bud frequencies in the peripheral blood lymphocytes of diesel engine exhaust-exposed workers. Toxicol Sci 143(2):408–417. https://doi.org/10.1093/toxsci/kfu239